

## 3D MR Sequence Capable of Simultaneous Image Acquisitions with and without Blood Vessel Suppression : Utility in Diagnosing Brain Metastases

菊地, 一史

<https://doi.org/10.15017/1500596>

---

出版情報 : 九州大学, 2014, 博士 (医学), 課程博士  
バージョン :  
権利関係 : やむを得ない事由により本文ファイル非公開 (2)



# **3D MR Sequence Capable of Simultaneous Image Acquisitions with and without Blood Vessel Suppression: Utility in Diagnosing Brain Metastases**

Kazufumi Kikuchi<sup>1</sup>, MD, Akio Hiwatashi<sup>1</sup>, MD, PhD, Osamu Togao<sup>1</sup>, MD, PhD, Koji Yamashita<sup>1</sup>, MD, PhD, Masami Yoneyama<sup>2</sup>, MT, Makoto Obara<sup>3</sup>, MS, Junji Kishimoto<sup>4</sup>, MS, Takashi Yoshiura<sup>1</sup>, MD, PhD, Hiroshi Honda<sup>1</sup>, MD, PhD

<sup>1</sup>Department of Clinical Radiology, Graduate School of Medical Sciences, Kyushu University

3-1-1 Maidashi, Higashi-ku, Fukuoka 812-8582, Japan

<sup>2</sup>Yaesu Clinic

C-road Bldg 4F, 2-1-18 Nihonbashi, Chuo-ku, Tokyo 103-0027, Japan

<sup>3</sup>Philips Electronics Japan

2-13-37, Konan, Minato-ku, Tokyo 108-8507, Japan

<sup>4</sup>Department of Research and Development of Next Generation Medicine, Faculty of Medical Sciences, Kyushu University

3-1-1 Maidashi, Higashi-ku, Fukuoka 812-8582, Japan

Corresponding author:

Akio Hiwatashi, MD, PhD

TEL: +81-92-642-5695

FAX: +81-92-642-5708

Email: hiwatasi@radiol.med.kyushu-u.ac.jp

**Original Article**

**Abstract:**

*Objective* Volume isotropic simultaneous interleaved bright- and black-blood examination (VISIBLE) is a recently developed 3D MR sequence that provides simultaneous acquisitions of images with blood vessel suppression (Black) and images without it (Bright). Our purpose was to evaluate the usefulness of VISIBLE in detecting brain metastases.

*Methods* This prospective study included patients with suspected brain metastasis imaged with both VISIBLE and MPRAGE. From dataset, we first compared the number of visualized blood vessels and the lesion-to-normal contrast-to-noise ratio (CNR) in 60 patients. We also performed an observer test to compare their diagnostic performance with VISIBLE, MPRAGE, and only Black in 34 patients. Diagnostic performance was evaluated using a figure of merit (FOM), sensitivity, false-positive results per case (FPs/case) and reading time.

*Results* The number of vessels was significantly fewer in Black compared to MPRAGE and Bright ( $P<0.0001$ ). CNR was significantly higher with both Black and Bright than with MPRAGE ( $P<0.005$ ). In the observer test, significantly higher sensitivity ( $P<0.0001$ ) and FOM ( $P<0.0001$ ), significantly shorter reading time

( $P=0.0001$ ), and similar FPs/case were achieved with VISIBLE compared to MPAGE. Compared to only Black, VISIBLE resulted in comparable sensitivity, but significantly fewer FPs/case ( $P=0.0008$ ).

*Conclusion* VISIBLE can improve radiologists' diagnostic performance for brain metastasis.

**Keywords:**

VISIBLE (Volume isotropic simultaneous interleaved bright- and black-blood examination)

Blood vessel suppression

Magnetic resonance imaging

Contrast-enhanced MRI

Metastatic brain tumor

**Key points:**

- VISIBLE can achieve higher sensitivity and shorter reading time than MPRAGE.
- VISIBLE can achieve fewer false positive rates than Blood vessel suppressed images.
- Compared to MPRAGE, VISIBLE can improve diagnostic performance for brain metastasis.

**Abbreviations and acronyms:**

3D            Three dimensional

ANOVA	Analysis of variance
CNR	Contrast-to-noise ratio
EPI	Echo-planar imaging
FA	Flip angle
FOM	Figure of merit
FOV	Field of view
FP	False-positive
FPS/case	False-positive results per case
GRE	Gradient-recalled echo
HSD	Honestly significant difference
iMSDE	Improved motion-sensitized driven-equilibrium
JAFROC	Jackknife free-response receiver operating characteristic
MPRAGE	Magnetization-prepared rapid acquisition of gradient echo
MSDE	Motion-sensitized driven-equilibrium
PACS	Picture archiving and communication system
ROI	Region of interest
SENSE	Sensitivity-encoding

SRS	Stereotactic radiosurgery
TE	Echo time
TFE	Turbo field-echo
TI	Inversion time
TR	Repetition time
TSE	Turbo spin-echo
TSE-MSDE	TSE with MSDE preparation
Venc	Velocity-encoding
VISIBLE	Volume isotropic simultaneous interleaved bright- and black-blood examination
WBRT	Whole brain radiation therapy

## Introduction

Brain metastasis is a common complication due to cancer [1, 2]. The accurate pretreatment diagnosis of brain metastasis is essential to the determination of the appropriate therapeutic strategy. For example, treatment with stereotactic radiosurgery (SRS) is considered if the patients have small (less than 3 cm in diameter) lesions with less than five in number, because the risk of radiation induced leukoencephalopathy with SRS is less than that with whole brain radiation therapy (WBRT). WBRT is a standard therapy for multiple intraparenchymal or leptomeningeal metastases. Due to the technical improvements of SRS, patients with a higher number of metastases can be treated successfully. Generally, an accurate pretreatment evaluation of the number and the size of the lesions is essential [3-7].

MR imaging — particularly post-contrast three-dimensional (3D) T1-weighted gradient-recalled echo (GRE) imaging — has been the gold standard test for detecting brain metastases [8-10]. However, in this sequence, enhancing blood vessels are visualized as high-signal-intensity areas, potentially mimicking metastatic tumors. Although the enhancing blood vessels can usually be discriminated from metastases based on their curvilinear shape, careful and often laborious reading is



required to achieve an accurate diagnosis. To solve this problem, imaging with blood vessel suppression (black-blood techniques) were introduced [11-15].

For example, Komada et al. [11] used a 3D turbo spin-echo (TSE) sequence with the variable flip angle (FA) echo-train technique, which resulted in blood vessel suppression. Nagao et al. [13] used a 3D TSE sequence implemented with a black-blood technique called motion-sensitized driven-equilibrium (MSDE) preparation (TSE-MSDE). With MSDE preparation, signals from flowing blood are selectively suppressed through phase-dispersion induced by flow-sensitizing gradients [16-20]. Nagao et al. [13] reported that TSE-MSDE could increase the sensitivity in detecting metastases and shorten the reading time compared to a conventional 3D GRE sequence. However, they warned insufficiently suppressed blood vessels could closely mimic metastatic tumors, which resulted in an increased false-positive (FP) rate with TSE-MSDE [13].

A new 3D MR sequence called volume isotropic simultaneous interleaved bright- and black-blood examination (VISIBLE) was recently proposed [21]. VISIBLE provides simultaneous acquisitions of images with blood vessel suppression ("Black images" hereafter) and without blood vessel suppression ("Bright images"). We

hypothesized with VISIBLE, both high sensitivity and a low FP rate could be achieved at the same time by using the Bright images in conjunction with the Black images. Thus, our purpose was to evaluate the usefulness of VISIBLE in detecting brain metastases by comparing VISIBLE with conventional GRE imaging.

## **Materials and Methods**

This prospective study was approved by the local institutional review board, and written informed consent was obtained from all participants before enrollment in the study.

### ***MR Imaging***

The technical details of VISIBLE have been reported [21]. Briefly, the VISIBLE sequence was based on 3D T1-turbo field-echo (T1-TFE) sequence. To suppress blood signals, this sequence has black-blood pre-pulse called motion sensitized driven equilibrium (MSDE). The MSDE pre-pulse comprises a series of radiofrequency (RF) pulses with  $90^\circ$ /  $180^\circ$ /  $-90^\circ$  flip angles (i.e., T2-prep pulse) and motion-sensitization gradients that are placed symmetrically around the  $180^\circ$  pulse.

Similar to the motion-probing gradients on single-shot echo-planar imaging (EPI)-based diffusion-weighted images that can effectively suppress the signal of flowing vessels, this pair of gradients at MSDE can also suppress vessels. The original MSDE preparation consists of a T2 preparation ( $90^\circ/180^\circ/-90^\circ$ ) pulses with motion-sensitizing gradients sandwiched in between the RF pulses. The iMSDE has been developed to address the sensitivity of MSDE to eddy currents and the inhomogeneity of MSDE image quality [17]. The iMSDE preparation consists of a  $90^\circ$  excitation pulse, two  $180^\circ$  Malcom-Levitt (MLEV) refocusing pulses and a  $-90^\circ$  flip-back pulse with motion-sensitizing gradients sandwiched between the RF pulses. Additional bipolar gradients inserted in front of the  $90^\circ$  excitation pulse work to compensate for eddy currents. After iMSDE preparation, two sequential phases of TFE were implemented. T1-TFE with MSDE can provide Black images, T1-TFE without MSDE can provide Bright images (Fig. 1).

All MR examinations were performed with a 3T scanner (Achieva TX; Philips Health Care, Best, the Netherlands) and an 8-channel head coil. For each patient, both VISIBLE and a conventional 3D GRE imaging (magnetization-prepared rapid acquisition of gradient echo, MPRAGE) were sequentially obtained after an intra-

venous administration of gadoteridol (ProHance; Eisai, Tokyo, Japan; 0.2 mmol/Kg).

The imaging parameters for the MPRAGE were repetition/echo time (TR/TE), 8.2/3.8 ms; inversion time (TI), 1028 ms; FA, 8°; and sensitivity-encoding (SENSE) factors, 1 (phase) and 2.5 (section). The imaging parameters for the VISIBLE were TR/TE, 6.9/3.2 ms; FA, 15°; TFE factor, 20; SENSE factors, 2 (phase) and 1.4 (section); and velocity-encoding (Venc) for MSDE, 6.0 mm/s. We set the Venc at the lowest available to maximize the blood vessel suppression. The imaging times were 5 min 20 s for MPRAGE and 5 min 8 s for VISIBLE.

Both the MPRAGE and VISIBLE images were obtained in a sagittal plane with the same field of view (240×240 mm<sup>2</sup>) and voxel size (1.0×1.0×1.0 mm<sup>3</sup>) and subsequently reformatted into 2-mm-thick contiguous transverse images. The first post-contrast scan was initiated at 5 min after the contrast injection. To avoid timing bias after contrast injection, we alternated the order of the two post-contrast sequences: VISIBLE was obtained first in the first imaging order (order 1 hereafter) and MPRAGE was first in the second imaging order (order 2).

### ***Database of Patient Images***

Between December 2011 and February 2013, we prospectively collected images of 478 consecutive head MR examinations of 366 patients with suspected brain metastasis to construct an image database. From the pooled images, patients with a history of pathologically proven cancer and with one or more follow-up MR examinations were selected. In our database, we excluded a total of 168 patients because there were no pathological confirmation of the primary cancer ( $n = 42$ ), the later revealed benign tumor ( $n = 18$ ), and no follow-up ( $n = 108$ ). In a consensus reading of images of those patients, two board-certified radiologists (K.K. and T.Y. with 6 and 25 years of experience in diagnostic radiology, respectively) identified intraparenchymal enhancing lesions that were visualized in both MPRAGE and VISIBLE. Enhancing lesions visualized in only one of the two types of images were excluded since they could possibly represent artifacts.

An intraparenchymal enhancing brain lesion was deemed metastasis when it satisfied either of the following conditions: 1) the lesion size increased in the follow-up examination, or 2) the lesion size decreased after radiotherapy or chemotherapy. As a result, 995 metastases were found in 116 MR examinations from 84 patients, while 119 head MR images from 114 patients were found to have no enhancing

lesions. In our database, the number of metastases were as follows 1 (n = 6), 2 (n = 3), 3 (n = 2), 4 (n = 3), 5 (n = 0), 6 (n = 3), 7 (n = 0), 8 (n = 0), 9 (n = 1), 10 (n = 1), >10 (n = 65).

### ***Evaluation of Image Quality***

We compared the number of blood vessels in three types of sequences; MPRAGE, Black images from VISIBLE and Bright images from VISIBLE. We also compared the lesion-to-normal contrast-to-noise ratio (CNR) among these three types of images. All of these evaluations were performed using a 20.8-inch liquid crystal display monitor of a picture archiving and communication system (PACS; Synapse PACS, Fujifilm, Tokyo, Japan). The number of blood vessels was counted in 20 patients with no enhancing lesion (13 men, 7 women; age, 41–85 years) scanned in order 1, and in another 20 patients with no enhancing lesion (11 men, 9 women; age, 37–83 years) in order 2 randomly selected patients from database. Therefore a total of 40 patients were selected from our database. A board-certified radiologist (K.K.) counted the numbers of enhancing blood vessels in a single centrum semioval section for each type of images.

For the evaluation of the CNR, metastatic lesions with homogeneous enhancement and a diameter greater than 5 mm were selected. As a result, 40 lesions from a total of 20 patients in our data base, including 20 imaged in order 1 from 10 patients (4 men, 6 women; age, 40–76 years; all patients with lung cancer) and 20 in order 2 from 10 patients (4 men, 6 women; age, 35–76 years; all patients with lung cancer) were used. The CNR was calculated by using the following formula:

$$\text{CNR} = (\text{SI}_{\text{lesion}} - \text{SI}_{\text{background}}) / 0.5 \times (\text{SD}_{\text{lesion}} + \text{SD}_{\text{background}})$$

where  $\text{SI}_{\text{lesion}}$  and  $\text{SI}_{\text{background}}$  represent the mean signal intensities of the enhancing lesion and normal-appearing white matter in the same section, respectively, and  $\text{SD}_{\text{lesion}}$  and  $\text{SD}_{\text{background}}$  are the corresponding standard deviations. These parameters were measured by a board-certified radiologist (K.K.) within a circular region of interest (ROI) with a diameter of 5 mm.

### ***Observer Tests***

From the image database, we selected patients with 1 to 6 metastases: 17 patients (8 men, 9 women; age, 57–84 years; 10 patients imaged in order 1 and 7 patients imaged in order 2; 14 patients with lung cancer, 1 with ureter cancer, 1 with

esophageal cancer and 1 with malignant mesothelioma) with 48 lesions. The longer diameter of each lesion was measured by a board-certified radiologist (K.K.). In addition, 17 patients without any enhancing lesions (8 men, 9 women; age, 57–84 years) were selected, matching their ages, genders and imaging order to the 17 cases with metastases. Images of these 34 patients were used for the observer tests.

Twelve observers including seven board-certified radiologists (6, 6, 10, 11, 12, 14 and 16 years of experience) and five radiology residents (two first-year, two second-year and one third-year) who were blinded to the patients' information took part in the observer tests. Each observer attended three reading sessions that were held at least 1 month apart to minimize learning effects: they read VISIBLE (both Black and Bright images), MPRAGE, and only Black images of VISIBLE in the first, the second and the third reading sessions, respectively. In each session, the observers used the PACS to read the images of the 34 cases that were presented in a randomized order.

The observers recorded the results of their reading by placing an arrow electronically at each location where they found a metastasis. They reported their level of confidence in the presence of metastasis at each location by assigning a



number ranging from 0 (lowest confidence level) to 100 (highest level). In the first reading session, in which VISIBLE was read, the observers were instructed beforehand to use the synchronized section increment function of the PACS so that they could compare the findings of Black and Bright images: they were asked to use Black images to screen for high-signal-intensity areas as candidates for metastases and Bright images as a second opinion to reject FPs such as enhancing vessels. The reading time was also recorded.

### ***Statistical Analyses***

We compared the number of blood vessels and CNR using the Tukey's honestly significant difference (HSD) test when the result of a two-way analysis of variance (ANOVA) was significant. The radiologists' performance in the observer test was evaluated using a figure of merit (FOM) derived from the jackknife free-response receiver operating characteristic (JAFROC) analysis with method 1 of Chakraborty and Berbaum [22, 23]. We also obtained the sensitivity and the number of FPs per case (FPs/case).

The FOM, sensitivity, FPs/case, and reading time were compared among the three reading sessions using the Tukey's HSD test when the result of a two-way ANOVA was significant. We also compared the sensitivity among the three sessions according to lesion size: small ( $\leq 5$  mm in longer diameter) and large ( $> 5$  mm). Imaging findings related to the FP results were judged by the consensus of the two board-certified radiologists (K.K. and T.Y.). For all analyses,  $P < 0.05$  was considered significant.

## **Results**

### ***Evaluation of Image Quality***

Figure 2 shows the number of enhancing blood vessels compared among the three types of images. The number of blood vessels was significantly fewer in the Black images from VISIBLE than in the MPRAGE and Bright images from VISIBLE ( $P < 0.0001$  for each comparison for both imaging orders). In the Bright images from VISIBLE, the number of blood vessels was recovered, although it was slightly fewer than that in the MPRAGE images ( $P = 0.0296$  for order 1,  $P = 0.0004$  for order 2).

Figure 3 shows the CNR compared among the three types of images. The CNRs

were significantly higher in the both Black and Bright images from VISIBLE compared to the MPRAGE images ( $P = 0.0003/0.0027$  in Black/Bright for order 1,  $P = 0.0003/0.0003$  in Black/Bright for order 2). No significant difference was seen between the Black and Bright images for either imaging order.

### ***Observer Tests***

The longer diameter of the 48 lesions used in the observer tests ranged from 1.5 to 43.2 mm (median, 2.9 mm, Fig. 4). There were 37 small ( $\leq 5$  mm in longer diameter) and 11 large ( $> 5$  mm) lesions. Table 1 summarizes the results of the observer tests. Among the board-certified radiologists and the residents, the sensitivity with VISIBLE (both Black and Bright images) and that with only Black images were significantly higher than that with MPRAGE ( $P < .0001$  for each comparison). No significant difference in sensitivity was observed between the VISIBLE and only Black images in any observer groups.

The FPs/case obtained with the only Black images (mean  $\pm$  standard deviation;  $0.521 \pm 0.283$ ) was significantly higher than those with VISIBLE ( $0.151 \pm 0.077$ ) among the board-certified radiologists ( $P = 0.0037$ ), however there were no

statistically significant difference with MPAGE ( $0.303 \pm 0.119$ ;  $P > 0.05$ ). The FPs/case obtained with the only Black images ( $0.485 \pm 0.282$ ) was significantly higher than those with VISIBLE ( $0.174 \pm 0.087$ ) and MPAGE ( $0.294 \pm 0.137$ ) among all 12 observers ( $P = 0.0008$  for the comparison with VISIBLE and  $P = 0.0456$  for the comparison with MPAGE), whereas no such difference was found among the residents ( $0.206 \pm 0.100$  for VISIBLE,  $0.282 \pm 0.175$  for MPAGE, and  $0.435 \pm 0.305$  for Black, respectively;  $P > 0.05$ ). No difference in FPs/case was found between VISIBLE and MPAGE in any observer groups ( $P > 0.05$ ).

The FOM with VISIBLE was significantly higher than that with MPAGE among all observer groups ( $P < .0005$  for all comparisons) and that with only Black images among residents ( $P = 0.0340$ ) and all observers ( $P = 0.0112$ ) whereas no difference was found among the board-certified radiologists. The FOM with the only Black images was significantly higher than that with MPAGE among all observer groups ( $P < .0001$  among the board certified radiologists and all observers,  $P = 0.0375$  among the residents).

The reading time with VISIBLE was significantly shorter than that with MPAGE among the board-certified radiologists ( $P < .0001$ ) and all observers ( $P =$

0.0001), whereas no significant difference was found among the residents. The reading time with the only Black images was significantly shorter than that with MPAGE among each observer group ( $P < .0001$  for each comparison), and it was significantly shorter than that with VISIBLE among the residents ( $P < .0001$ ) and all observers ( $P < 0.0015$ ), but not among the board-certified radiologists.

Table 2 shows the sensitivities according to the lesion size. In detecting small ( $\leq 5$  mm) lesions, the sensitivities obtained with VISIBLE (84.9%–85.7%) and with only Black images (81.1%–86.5%) were much higher than those with MPAGE (56.2%–63.3%;  $P < .0001$  for each comparison). On the other hand, in detecting large ( $> 5$  mm) lesions, the sensitivities obtained with all three methods were nearly 100%, although a few false-negatives with MPAGE resulted in significantly lower sensitivity compared to the VISIBLE and only Black images ( $P = 0.0456$ ,  $0.0277$ , and  $0.0008$  for among the board-certified radiologists, residents, and all observers, respectively).

Table 3 summarizes the image findings related to FP results. In all three sessions, vessels were the most frequent sources of FP findings. The frequency of FPs originating from vessels was greatly reduced in the reading with VISIBLE (62

FPs) compared to the reading with only Black images (182 FPs) among all 12 observers.

Figure 5 shows a representative case with metastases imaged with VISIBLE and MPAGE.

## **Discussion**

Our observer tests showed the FOM with VISIBLE (both Black and Bright images) was significantly higher than that with MPAGE among both board-certified radiologists and residents (Table 1), indicating that VISIBLE may improve radiologists' performance in detecting brain metastases. Notably, the FOM with VISIBLE was the highest among the three types of images for each of the 12 observers. The high diagnostic performance with VISIBLE resulted primarily from high sensitivity. Similar to the FOM results, the sensitivity with VISIBLE was higher than that with MPAGE for each of the 12 observers, including both board-certified radiologists and residents (Table 1).

Moreover, VISIBLE was found to be especially useful for detecting small ( $\leq 5$  mm) metastatic lesions (Table 2). Indeed, among the residents a prominent

improvement in sensitivity to small lesions was shown with VISIBLE (84.9%) compared to that with MPAGE (56.2%). Since, in the reading session with VISIBLE, each observer was instructed to use Black images to pick up high-signal-intensity areas as candidates for metastases, it is conceivable that the higher sensitivity with VISIBLE compared to MPAGE was due to blood vessel suppression by the MSDE preparation and the higher CNR of Black images revealed in the evaluation of image quality (Figs. 2 and 3). The underlying mechanism for higher CNRs with VISIBLE than with MPAGE is subject to further investigation, but it may be accounted for by the magnetization transfer effect induced by MSDE pre-pulses which resulted in the suppression of the background signal of brain parenchyma, especially the white matter.

The absence of a significant difference in FPs/case between VISIBLE and MPAGE (Table 1) supports our hypothesis that referring to Bright images as a second opinion would exclude FPs due to insufficiently suppressed blood vessels in Black images. This was confirmed by our finding that the FPs/case with VISIBLE was significantly lower than that with only Black images among the board-certified radiologists and all 12 observers (Table 1). Furthermore, the frequency of the FPs

originating from vessels was greatly reduced with VISIBLE compared to only Black images (Table 3).

In a previous report, FPs due to insufficiently suppressed blood vessels in TSE-MSDE were excluded by combined reading with MPRAGE [13]. However, this required an additional acquisition of MPRAGE, which resulted in prolonged imaging time. It is notable VISIBLE allows for the acquisition of both Black and Bright images within approximately 5 min. It should be also noted that the two types of images are precisely matched in geometry since they are acquired simultaneously after each excitation. This feature facilitates easy comparisons between Black and Bright images on a PACS. Figures 6 and 7 show illustrative cases in which a false-positive due to an insufficiently suppressed blood vessel on Black images was successfully excluded by Bright images. Only using Black images for detecting brain metastasis, we will mistake insufficient suppressed vessels for metastases, especially slow flowing veins. This may be the drawback of VISIBLE sequence.

The reading time with VISIBLE was significantly shorter than that with MPRAGE among the board-certified radiologists and among all 12 observers (Table 1). This suggests the radiologists' reading process was simplified with VISIBLE



despite the fact that it includes the reading of two sets of images. On the other hand, no significant difference in reading time was found between VISIBLE and MPAGE among the residents (Table 1). We speculate the residents were less skillful at the integration of findings from Black and Bright images compared to the board-certified radiologists. Nevertheless, it should be noted that the residents' mean reading time with VISIBLE was not longer than that with MPAGE.

This study has several limitations. First, no pathological diagnosis was obtained for the brain metastases. The possible contamination of other types of lesions such as subacute infarction cannot be completely excluded. However, as this study focuses on lesion detection, this might not be a substantial limitation. Second, although the number of blood vessels on the Bright images was substantially recovered compared to that on the Black images, it is still significantly lower than that on MPAGE (Fig. 2). The lack of delineation of fine vessels on Bright images might lead to a failure of rejecting FPs due to insufficiently suppressed blood vessels on Black images. Nevertheless, our observer test revealed no significant increase in FPs/case with VISIBLE. Thus we believe the degree of blood vessel visualization on Bright images is practically acceptable. Third, a direct comparison with recently

available 3D TSE techniques [11, 13, 15] was not performed, to avoid extended examination times. We observed the improved specificity of VISIBLE compared to TSE-MSDE shown by the comparable FPs/case with MPRAGE, which resulted in fewer FPs/case than TSE-MSDE in a previous report [13]. However, 3D TSE techniques are reportedly associated with higher CNRs than GRE techniques [11, 13], as was the case with VISIBLE in the present study. Thus the relative merits of VISIBLE and TSE-MSDE regarding CNR and sensitivity are unpredictable. Finally, enhancing lesions visualized by only VISIBLE or only MPRAGE were not included in the analysis, to minimize the chance of contamination from artifacts. Metastatic lesions visualized only by VISIBLE which had higher CNR might have been excluded.

In conclusion, with increased sensitivity and comparable specificity, VISIBLE can improve radiologists' diagnostic performance for brain metastasis compared with MPRAGE. In addition, VISIBLE can shorten experienced radiologists' reading time.

### **Conflict of Interest**

Makoto Obara is an employee of Philips Electronics Japan. He was not involved in data analysis in this study



## References

- 1 Posner JB, Chernik NL (1978) Intracranial metastases from systemic cancer.  
  
Adv Neurol 19:579-592
- 2 Rosner D, Nemoto T, Pickren J, Lane W (1983) Management of brain  
  
metastases from breast cancer by combination chemotherapy. J Neurooncol  
  
1:131-137
- 3 Linskey ME, Andrews DW, Asher AL et al (2010) The role of stereotactic  
  
radiosurgery in the management of patients with newly diagnosed brain  
  
metastases: a systematic review and evidence-based clinical practice  
  
guideline. J Neurooncol 96:45-68
- 4 Lippitz B, Lindquist C, Paddick I, Peterson D, O'Neill K, Beaney R (2014)  
  
Stereotactic radiosurgery in the treatment of brain metastases: the current  
  
evidence. Cancer Treat Rev 40:48-59
- 5 Monaco EA, 3rd, Faraji AH, Berkowitz O et al (2013) Leukoencephalopathy  
  
after whole-brain radiation therapy plus radiosurgery versus radiosurgery  
  
alone for metastatic lung cancer. Cancer 119:226-232

- 6 Serizawa T, Hirai T, Nagano O et al (2010) Gamma knife surgery for 1-10 brain metastases without prophylactic whole-brain radiation therapy: analysis of cases meeting the Japanese prospective multi-institute study (JLGK0901) inclusion criteria. J Neurooncol 98:163-167
- 7 Hunter GK, Suh JH, Reuther AM et al (2012) Treatment of five or more brain metastases with stereotactic radiosurgery. Int J Radiat Oncol Biol Phys 83:1394-1398
- 8 Schellinger PD, Meinck HM, Thron A (1999) Diagnostic accuracy of MRI compared to CCT in patients with brain metastases. J Neurooncol 44:275-281
- 9 Kakeda S, Korogi Y, Hirai Y et al (2007) Detection of brain metastasis at 3T: comparison among SE, IR-FSE and 3D-GRE sequences. Eur Radiol 17:2345-2351
- 10 Takeda T, Takeda A, Nagaoka T et al (2008) Gadolinium-enhanced three-dimensional magnetization-prepared rapid gradient-echo (3D MP-RAGE) imaging is superior to spin-echo imaging in delineating brain metastases. Acta Radiol 49:1167-1173

- 11 Komada T, Naganawa S, Ogawa H et al (2008) Contrast-enhanced MR imaging of metastatic brain tumor at 3 tesla: utility of T(1)-weighted SPACE compared with 2D spin echo and 3D gradient echo sequence. *Magn Reson Med Sci* 7:13-21
- 12 Kato Y, Higano S, Tamura H et al (2009) Usefulness of contrast-enhanced T1-weighted sampling perfection with application-optimized contrasts by using different flip angle evolutions in detection of small brain metastasis at 3T MR imaging: comparison with magnetization-prepared rapid acquisition of gradient echo imaging. *AJNR Am J Neuroradiol* 30:923-929
- 13 Nagao E, Yoshiura T, Hiwatashi A et al (2011) 3D turbo spin-echo sequence with motion-sensitized driven-equilibrium preparation for detection of brain metastases on 3T MR imaging. *AJNR Am J Neuroradiol* 32:664-670
- 14 Park J, Kim EY (2010) Contrast-enhanced, three-dimensional, whole-brain, black-blood imaging: application to small brain metastases. *Magn Reson Med* 63:553-561
- 15 Yoneyama M, Nakamura M, Tabuchi T et al (2013) Whole-brain black-blood imaging with magnetization-transfer prepared spin echo-like contrast: a novel

- sequence for contrast-enhanced brain metastasis screening at 3T. Radiol Phys Technol 6:431-436
- 16 Wang J, Yarnykh VL, Hatsukami T, Chu B, Balu N, Yuan C (2007) Improved suppression of plaque-mimicking artifacts in black-blood carotid atherosclerosis imaging using a multislice motion-sensitized driven-equilibrium (MSDE) turbo spin-echo (TSE) sequence. Magn Reson Med 58:973-981
- 17 Wang J, Yarnykh VL, Yuan C (2010) Enhanced image quality in black-blood MRI using the improved motion-sensitized driven-equilibrium (iMSDE) sequence. J Magn Reson Imaging 31:1256-1263
- 18 Dong L, Wang J, Yarnykh VL et al (2010) Efficient flow suppressed MRI improves interscan reproducibility of carotid atherosclerosis plaque burden measurements. J Magn Reson Imaging 32:452-458
- 19 Yuan C, Wang J, Balu N (2012) High-field atherosclerotic plaque magnetic resonance imaging. Neuroimaging Clin N Am 22:271-284, xi
- 20 Obara M, Kuroda K, Wang J et al (2013) Comparison between two types of improved motion-sensitized driven-equilibrium (iMSDE) for intracranial black-blood imaging at 3.0 tesla. J Magn Reson Imaging. 10.1002/jmri.24430

- 21 Yoneyama M, Obara M, Takahara T et al Volume isotropic simultaneous interleaved black-blood and bright-blood imaging: a novel sequence for contrast-enhanced brain metastasis screening. Magn Reson Med Sci in press.  
10.2463/mrms.2013-0065
- 22 Chakraborty DP, Berbaum KS (2004) Observer studies involving detection and localization: modeling, analysis, and validation. Med Phys 31:2313-2330
- 23 Chakraborty DP (2006) Analysis of location specific observer performance data: validated extensions of the jackknife free-response (JAFROC) method. Acad Radiol 13:1187-1193



## Figure Captions

**Fig. 1:** Diagram of the VISIBLE sequence. Two phases of TFE acquisition are implemented after iMSDE preparation. The first phase is for imaging with blood vessel suppression (Black images). The second phase, where the blood signal is recovered, is for imaging without blood vessel suppression (Bright images). The iMSDE preparation has a  $90^\circ$  excitation pulse, two  $180^\circ$  refocusing pulses, and a  $-90^\circ$  flip-back pulse. Each refocusing pulse is sandwiched by bipolar motion-sensitized gradients inserted in all three (x, y, and z) directions.

Note: ACQ = acquisition, G = gradient, iMSDE = improved motion-sensitized driven-equilibrium, RF = radiofrequency, TFE = turbo field-echo

**Fig. 2:** The number of enhancing blood vessels compared among the MPRAGE and Black and Bright images of VISIBLE obtained in order 1 (A) and order 2 (B).

Statistically significant differences were revealed among the three imaging methods.

Notably, the number of blood vessels is greatly reduced in the Black images whereas it is recovered in the Bright images.

**Fig. 3:** Lesion-to-normal CNRs for metastatic lesions compared among the MPRAGE and Black and Bright images of VISIBLE obtained in order 1 (A) and order 2 (B).

Statistically significant differences were seen between the MPRAGE and Black images as well as between the MPRAGE and Bright images, whereas no significant difference was observed between the Black and Bright images.

Note: NS = not significant

**Fig. 4:** The distribution of the 48 metastatic lesions used in the observer study according to lesion longer diameter.

**Fig. 5:** A 70-year-old woman with lung cancer and multiple brain metastases scanned in order 1 (VISIBLE first). In the right occipital lobe, the metastatic lesion (arrowhead) is more conspicuous in VISIBLE (Black and Bright images) than in MPRAGE. A tiny lesion in the left frontal lobe (arrow) is also more clearly visualized in VISIBLE than in MPRAGE. Note that blood vessels including meningeal vessels

are suppressed in the Black image, whereas they are almost completely restored in the Bright image.

**Fig. 6:** A 60-year-old woman with lung cancer. In the Black images, there is a small enhancing region in the right occipital lobe (arrows), which resembles a metastasis. In the Bright images, this enhancing region is confirmed as a part of a cortical vein based on its curvilinear shape (arrowheads).

**Fig. 7:** A 60-year-old woman with lung cancer. In the Black images, there is an enhancing region in the left frontal lobe (arrows). The Bright images reveal that it is a portion of medullary venous malformation insufficiently suppressed by iMSDE (arrowheads).

**Table 1.** Results of observer tests to compare VISIBLE and MPRAGE.

Observer	Sensitivity (%)			<i>P</i> -value*
	VISIBLE	MPRAGE	Black	
Board-certified radiologists				
A	87.5	66.7	83.3	< .0001/< .0001/0.9756
B	91.7	81.3	91.7	
C	91.7	75.0	95.8	
D	85.4	77.1	85.4	
E	95.8	79.2	95.8	
F	87.5	58.3	87.5	
G	83.3	58.3	87.5	
Mean±SD	89.0±4.3	70.8±9.7	89.6±5.0	
Residents				
H	89.6	51.2	79.2	
I	83.3	62.5	87.5	
J	91.7	72.9	85.4	

K	89.6	66.7	91.7	
L	87.5	66.7	85.4	
<b>Mean±SD</b>	88.3±3.2	64.0±8.1	85.8±4.5	< .0001/< .0001/0.7612
<b>All observers</b>				
<b>Mean±SD</b>	88.7±3.7	68.0±9.4	88.0±5.0	< .0001/< .0001/0.9471

---

\**P*-values are for comparisons between VISIBLE and MPRAGE / MPRAGE and Black / VISIBLE and Black.

**Table 1. cont'd** Results of observer tests to compare VISIBLE and MPAGE.

Observer	FOM			<i>P</i> -value*
	VISIBLE	MPRAGE	Black	
Board-certified radiologists				
A	0.926	0.773	0.894	
B	0.952	0.828	0.918	
C	0.953	0.826	0.920	
D	0.915	0.832	0.883	
E	0.944	0.868	0.919	
F	0.917	0.762	0.888	
G	0.900	0.722	0.884	
Mean±SD	0.930±0.020	0.802±0.051	0.901±0.017	< .0001/< .0001/0.1869
Residents				
H	0.919	0.754	0.875	

I	0.901	0.775	0.869	
J	0.917	0.819	0.892	
K	0.919	0.731	0.741	
L	0.923	0.779	0.838	
<b>Mean±SD</b>	0.916±0.009	0.772±0.033	0.843±0.060	0.0003/0.0375/0.0340
<b>All observers</b>				
<b>Mean±SD</b>	0.924±0.017	0.789±0.045	0.877±0.049	< .0001/< .0001/0.0112

---

\**P*-values are for comparisons between VISIBLE and MPRAGE / MPRAGE and Black / VISIBLE and Black.

**Table 1. cont'd** Results of observer tests to compare VISIBLE and MPRAGE.

Observer	Reading Time (s)			P-value*
	VISIBLE	MPRAGE	Black	
Board-certified radiologists				
A	67.6	81.8	52.9	
B	150.0	161.5	158.5	
C	138.4	200.0	162.4	
D	38.4	93.4	32.1	
E	121.2	163.6	130.9	
F	65.4	84.9	88.9	
G	96.3	82.8	76.9	
Mean±SD	96.8±41.6	124.0±49.5	100.4±51.2	< .0001/0.0004/0.8276
Residents				
H	76.2	74.1	55.6	
I	151.6	179.9	105.1	



J	104.4	112.4	70.1	
K	123.1	118.4	62.7	
L	81.1	66.9	44.1	
<b>Mean±SD</b>	107.3±31.1	110.3±45.0	67.5±23.1	0.7917/< .0001/< .0001
<b>All observers</b>				
<b>Mean±SD</b>	101.1±36.4	118.3±46.1	86.7±43.7	0.0001/< .0001/0.0015

---

\**P*-values are for comparisons between VISIBLE and MPRAGE / MPRAGE and Black / VISIBLE and Black.

**Table 2.** Comparison of the sensitivity of the three imaging methods according to the lesion size

	<b>VISIBLE</b>	<b>MPRAGE</b>	<b>Black</b>	<b><i>P</i>-value*</b>
<b>Board-certified</b>				
<b>radiologists</b>				
Diameter ≤ 5 mm	85.7	63.3	86.5	0.0003/0.0002/0.9844
> 5 mm	100	96.1	100	0.0456/0.0456/1.0000
<b>Residents</b>				
Diameter ≤ 5 mm	84.9	56.2	81.1	< .0001/< .0001/0.5666
> 5 mm	100	94.5	100	0.0277/0.0277/1.0000
<b>All observers</b>				
Diameter ≤ 5 mm	85.4	60.4	84.2	< .0001/< .0001/0.9315
> 5 mm	100	95.5	100	0.0008/0.0008/1.0000

Note. - Data are percentages.

\**P*-values for comparisons between VISIBLE and MPRAGE / MPRAGE and Black / VISIBLE and Black.



**Table 3.** Imaging findings related to false-positive results for the three imaging methods

Observers	Board-certified radiologists			Residents			All observers		
	VISIBLE	MPRAGE	Black	VISIBLE	MPRAGE	Black	VISIBLE	MPRAGE	Black
<b>Findings</b>									
Vessels	31	51	115	31	38	67	62	89	182
Artifacts	4	21	3	3	9	2	7	30	5
Choroid plexus	1	0	5	1	1	4	2	1	9
Others	0	0	1	0	0	1	0	0	2
<b>Total</b>	36	72	124	35	48	74	71	120	198

Note. - The numbers are the frequencies of the findings observed in each reading session.

Fig. 1

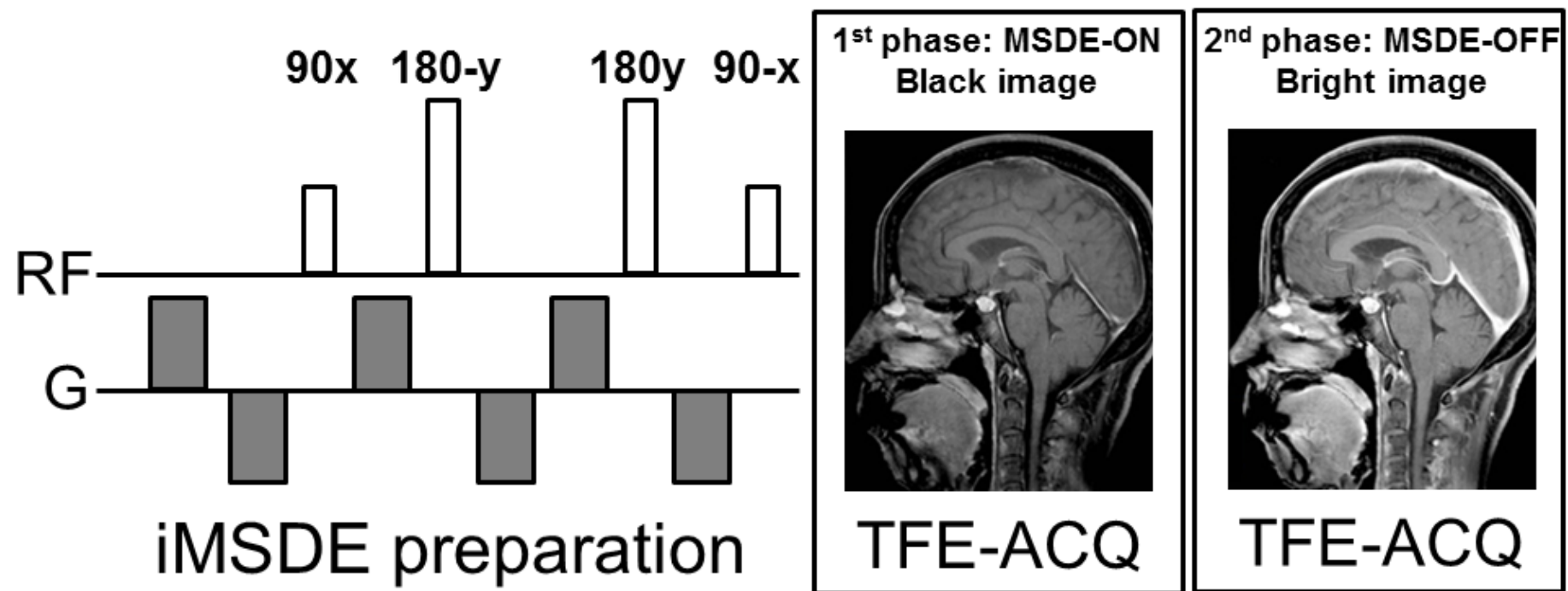


Fig. 2

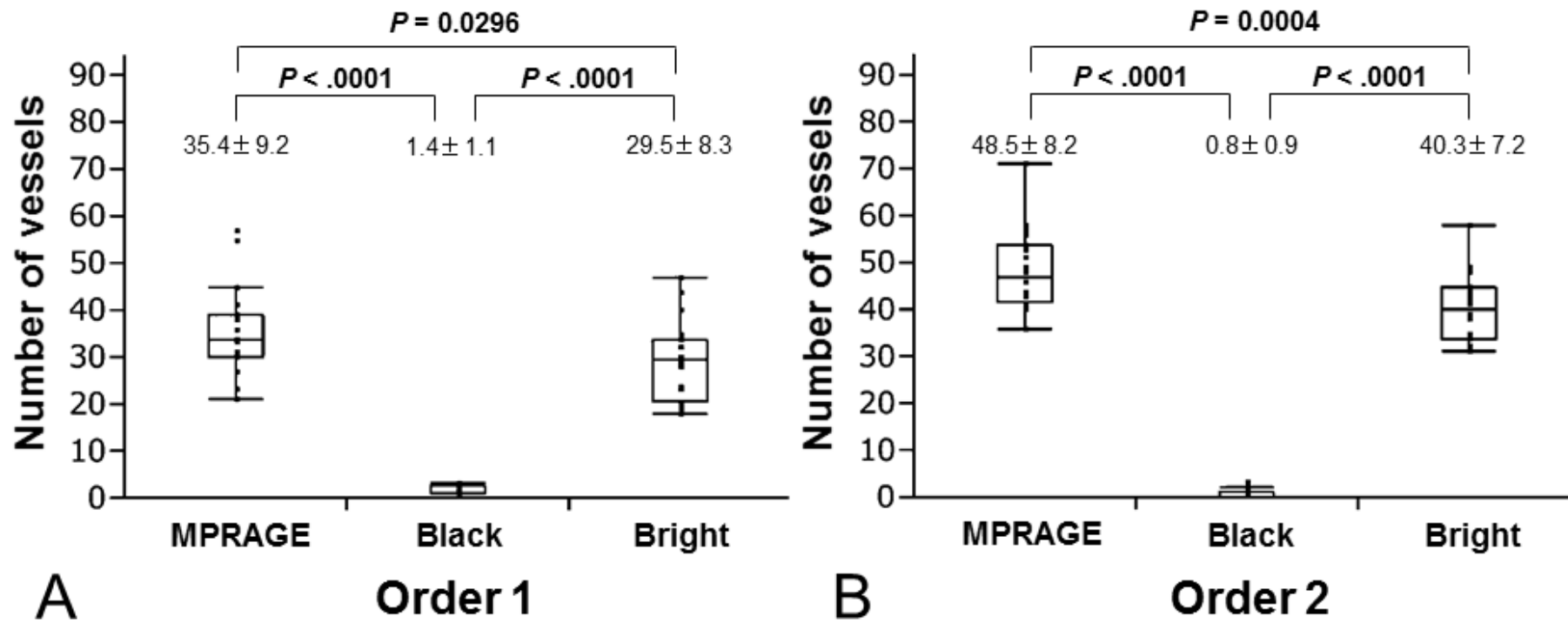


Fig. 3

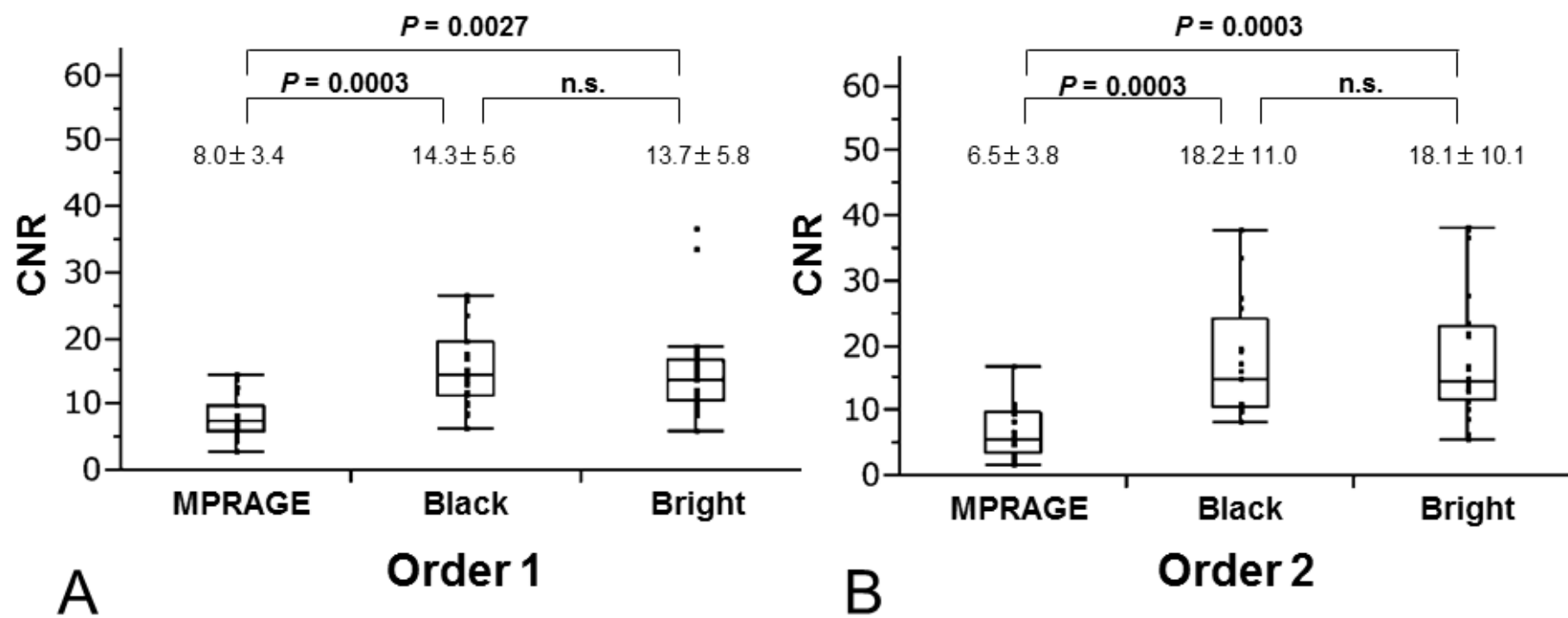


Fig. 4

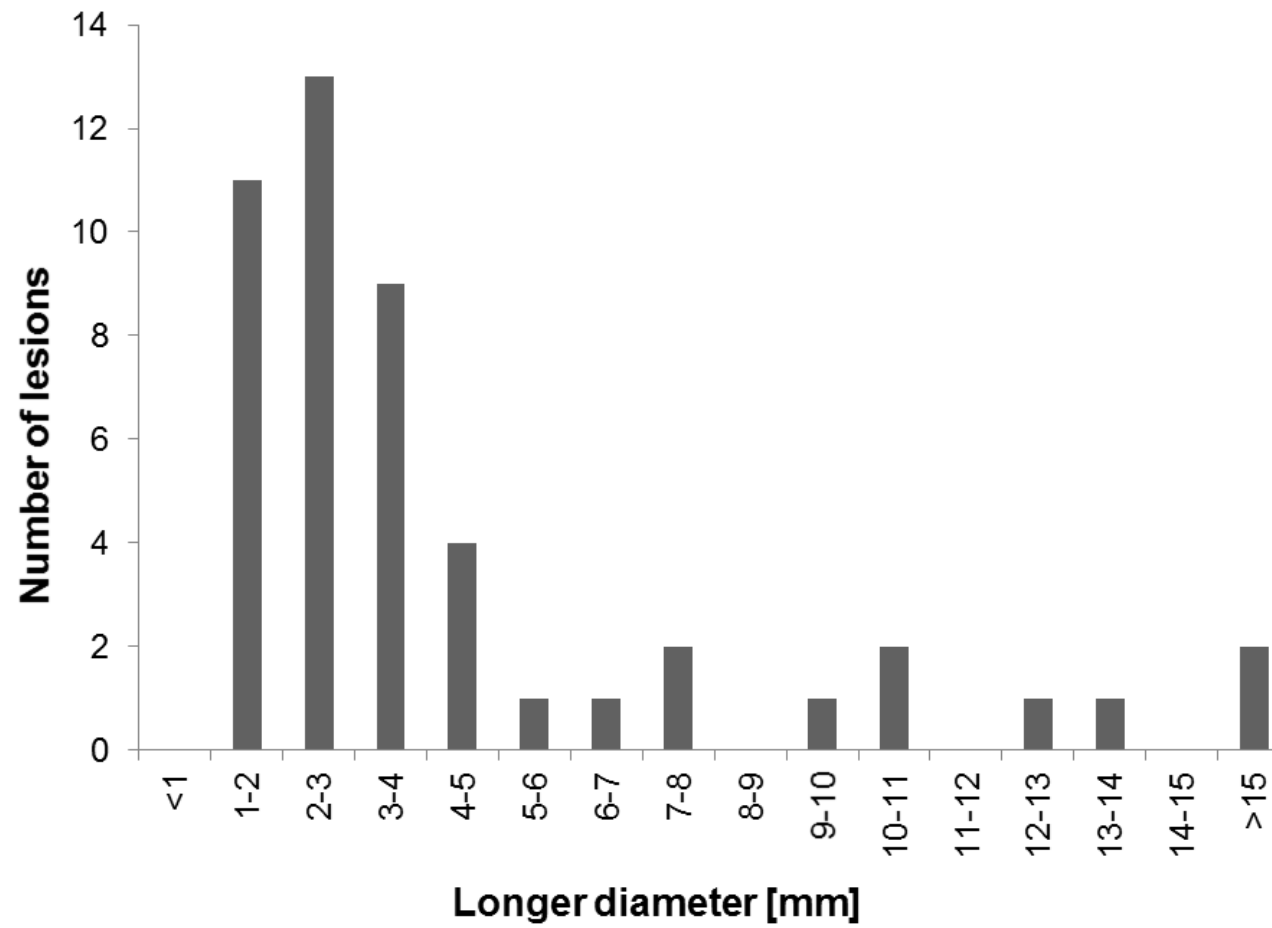




Fig. 5

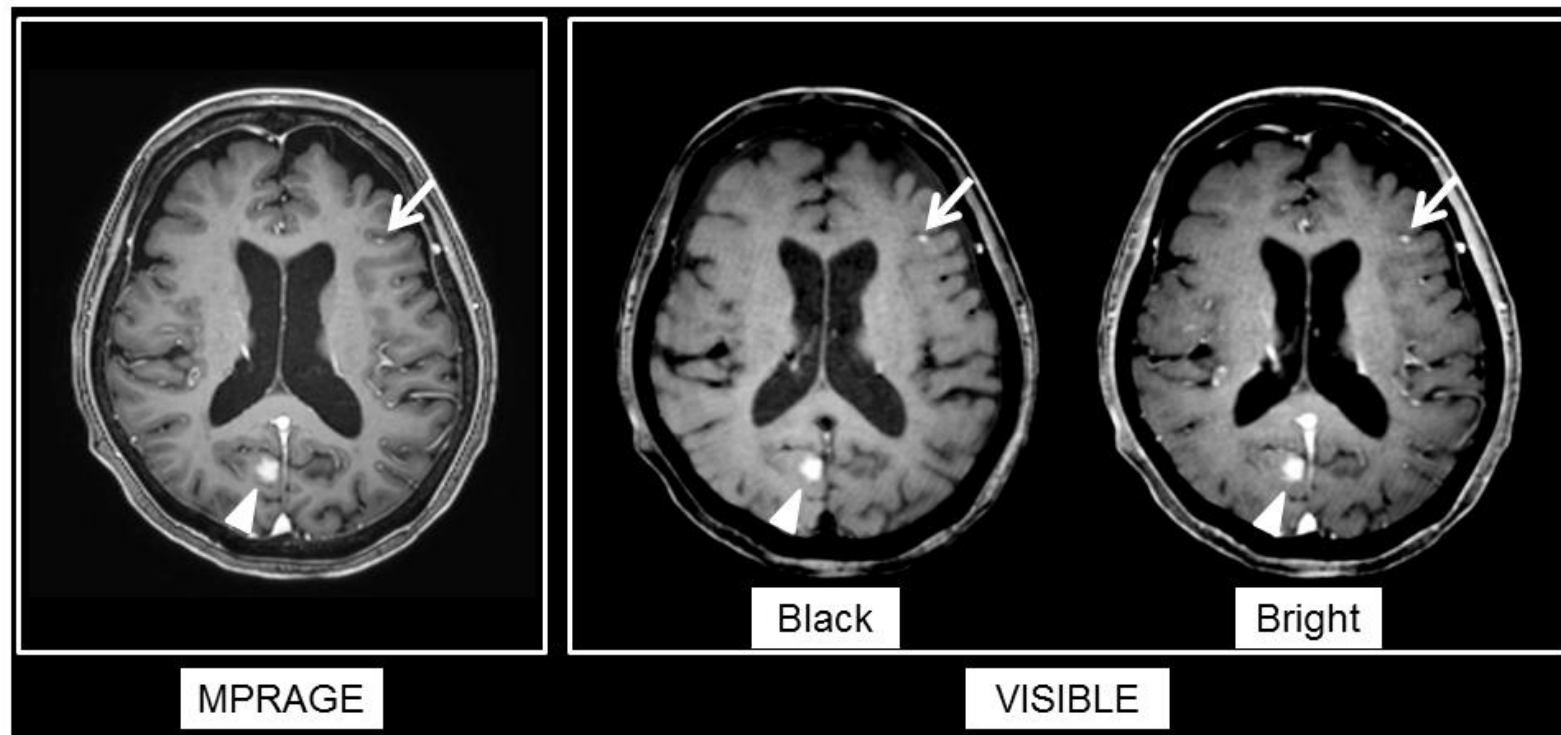


Fig. 6

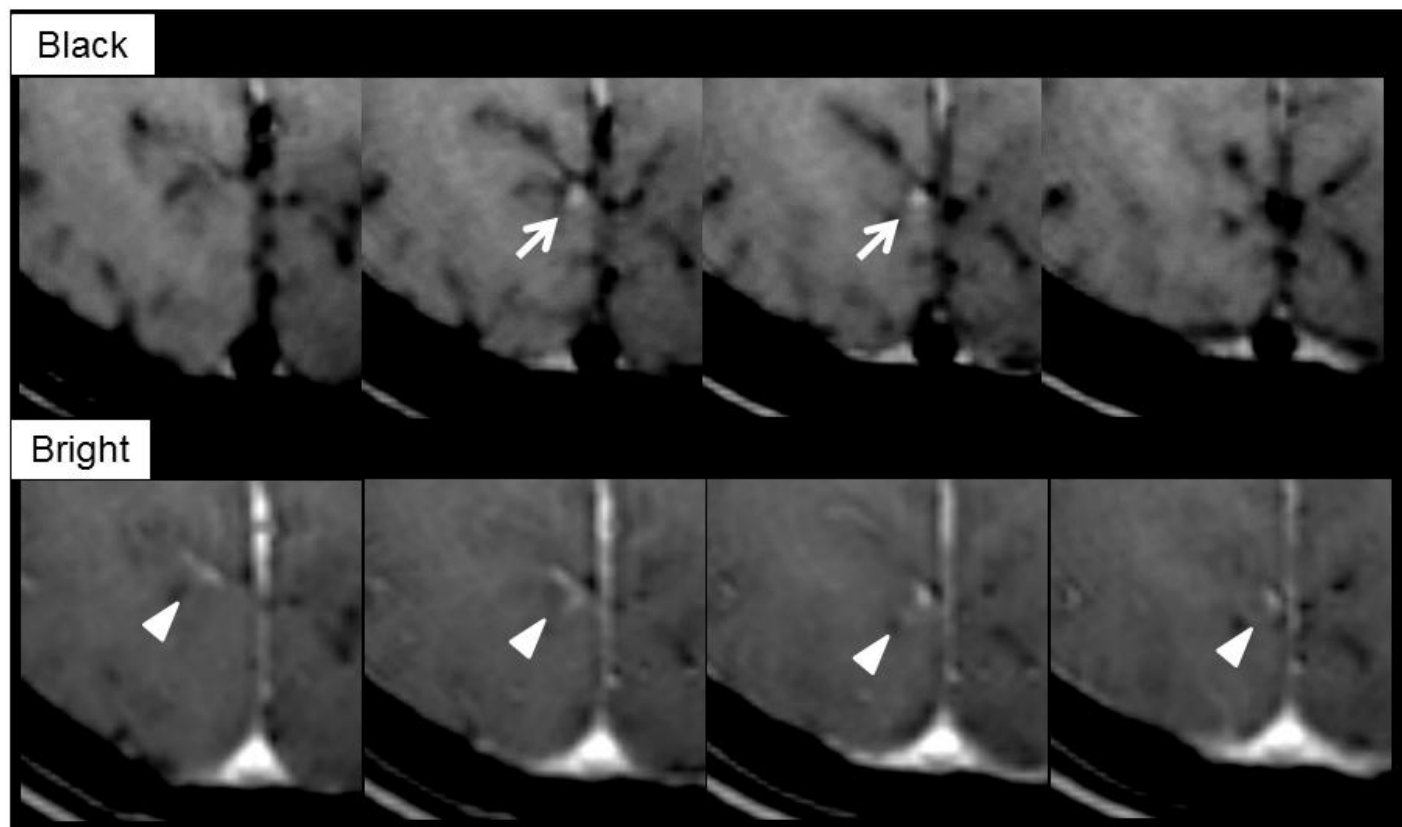


Fig. 7

